

CHAPTER 65

ANALYSIS OF THE FLOW INDUCED BY AIR-BUBBLE SYSTEMS

by

Helmut E. Kobus, Ph.D.

Research Engineer,

Versuchsanstalt für Wasserbau und Schiffbau

Berlin, Germany

ABSTRACT

The pattern of vertical velocities induced by an orifice discharging air into water can be represented by Gaussian distribution curves with a linear spread in the vertical except for the regions near the orifice and close to the free surface. An analytical treatment considering the momentum-flux increase due to the buoyancy of the air together with experimental information about the spread of the velocity profiles and the mean rising speed of the air bubble stream, which has been obtained from velocity and density measurements over a wide range of conditions, leads to a complete description of the flow field. The ratio of the water volume flux to the air discharge rate, which has been proposed as an efficiency criterion, is now at hand as a function of depth and air supply for both single orifices and rows. The experimental evidence supports the analysis well and suggests that extrapolation to larger water depths and air supplies should be permissible, which would allow approximate predictions of the volume flux for any air-bubble system.

INTRODUCTION

In recent years, air-bubble systems have been applied successfully as breakwaters and barriers against spreading of oil, salt water intrusion and ice formation. However, all attempts to correlate results from model tests and from field investigations have failed, because no analytical framework is at hand which suits both model and prototype. In a first attempt to close this gap, the vertical velocity field of the air-water mixture above an orifice has been measured and analyzed. The flow pattern produced by an air jet entering vertically into sideways unlimited water shows certain similarities to a submerged water jet [1] which suggest a similar analytical treatment with proper consideration of the momentum-flux increase with height due to the buoyancy of the air [2].

ANALYSIS

The air bubble stream

Consider an air jet discharging vertically upward at depth h below the water surface through a nozzle of diameter d_0 at a mass discharge rate Q_0 , pressure p_0 and density ρ_a^0 . If Ψ_0 is defined to be the volume flux corresponding to Q_0 at atmospheric pressure, then the momentum flux is given by

$$M_0 = \frac{(\rho_a^{\text{atm}} \Psi_0)^2}{\rho_a^0 \pi d_0^2 / 4} = \rho_a^{\text{atm}} \left(\frac{P_{\text{atm}}}{P_0} \right) \frac{\Psi_0^2}{\pi d_0^2 / 4} \quad (1)$$

or, in terms of a theoretical (loss-free) exit velocity U_0 and a discharge coefficient C_D , by

$$M_0 = C_D U_0 \rho_a^{\text{atm}} \Psi_0 \quad (2)$$

The continuous air stream discharging through the orifice quickly expands according to the sudden pressure drop across the nozzle and breaks up into bubbles of discrete size. It has been shown [5] that the bubble size distribution depends solely upon the discharge rate and varies neither with the fluid properties nor with the orifice diameter for all practical cases.

The speed of rise of the bubble stream rapidly approaches some terminal mean velocity \bar{U}_b . Fig.2 gives an indication of the extent of the "initial region", in which the local conditions at the orifice influence the flow pattern. Beyond this region, the bubble stream rises with a mean velocity \bar{U}_b determined by the bubble size distribution and concentration, which are both functions of the discharge rate Ψ_0 only. Therefore, \bar{U}_b should be a unique function of Ψ_0 independent of the local orifice conditions, which is confirmed by the experiments.

Extensive measurements on single bubbles so far have shown no evidence that the speed of rise varies considerably with the depth of submergence, although the change in bubble volume with depth or pressure would suggest so. But, except for very small bubbles, the speed of rise changes only gradually with the bubble diameter, which in turn changes only with the third root of the bubble volume or the local pressure. It is therefore considered a satisfactory approximation to assume the average rate of rise \bar{U}_b of the bubble stream to be independent of height.

The increment in buoyant force exerted upon the water by the air bubbles contained in a horizontal slice of thickness dx is given by the product of the air volume contained and the difference in specific weight. With

$$h^* = h + P_{\text{atm}}/\gamma_w \quad (3)$$

the air density at cross section x can be expressed as

$$\rho_a^x = \frac{\rho_a^{\text{atm}}}{P_{\text{atm}}} \gamma_w (h^* - x)$$

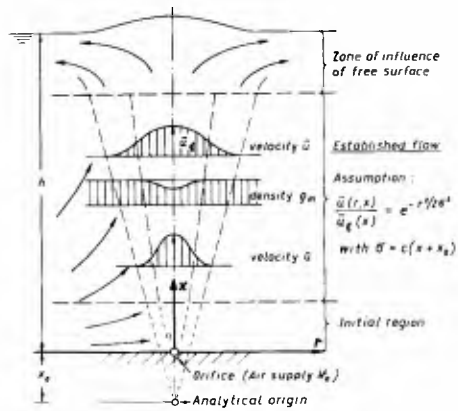


Fig.1 Definition Sketch

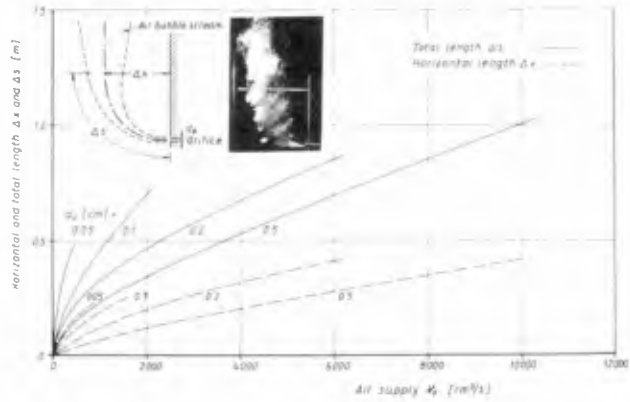


Fig.2 Initial Region

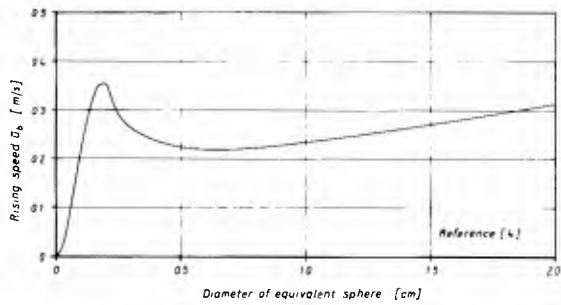


Fig.3 Rising Speed of Single Bubbles

and the increment in buoyant force is given by

$$dF(x) = \frac{Q_0}{\rho_a^x} \frac{dx}{\bar{u}_b} (\gamma_w - \gamma_a) = \frac{\rho_{atm} \psi_0}{\bar{u}_b (h^* - x)} \frac{(\gamma_w - \gamma_a)}{\gamma_w} dx$$

The buoyant force acting between the orifice and cross section x is then (with $\gamma_w - \gamma_a \approx \gamma_w$)

$$F(x) = \frac{\rho_{atm} \psi_0}{\bar{u}_b} \int_0^x \frac{dx}{h^* - x} = - \frac{\rho_{atm} \psi_0}{\bar{u}_b} \ln(1 - x/h^*)$$

and the total momentum flux at cross section x is now given by the sum of initial momentum flux and buoyant force,

$$M(x) = \rho_a^{atm} c_D U_0 \psi_0 - \frac{\rho_{atm} \psi_0}{\bar{u}_b} \ln(1 - x/h^*) \tag{4}$$

It is seen that the buoyancy term grows rapidly with distance x from the orifice while the contribution due to the initial momentum soon becomes negligible. The term M_0 can be neglected, if

$$\frac{\rho_a^{atm} c_D U_0 \psi_0}{-\frac{\rho_{atm} \psi_0}{\bar{u}_b} \ln(1 - x/h^*)} \approx \left(\frac{\rho_a^{atm}}{\rho_{atm}} \right) \frac{c_D U_0 \bar{u}_b}{x/h^*} \ll 1$$

Since, from the ideal gas law,

$$\rho_{atm} / \rho_a^{atm} = g RT \approx 90\,000 \text{ [m}^2/\text{s}^2]$$

and since U_0 cannot exceed the speed of sound (333 m/s), c_D is roughly 2/3, and \bar{u}_b is of the order of magnitude of 1 m/s, this condition results in

$$\frac{h^*}{500 x} \ll 1 \quad \text{or} \quad x \gg \frac{h^*}{500} \tag{5}$$

So, for instance, for M_0 to be less than 2 % of $M(x)$, x must be larger than $h^*/10$, which is a limit usually within the initial region. Beyond this lower limit, the momentum flux can be approximated by

$$M(x) = - \frac{\rho_{atm} \psi_0}{\bar{u}_b} \ln(1 - x/h^*) \tag{6}$$

Single orifice (axisymmetric case)

The analysis is based on two assumptions about the form of the velocity profiles : firstly, that the velocity profile at any horizontal section can be described by a Gaussian distribution curve,

$$u(r,x) = u_{\phi}(x) e^{-r^2/2\sigma^2}$$

and secondly, that these profiles are similar with respect to an "analytical origin" located at x_0 ,

$$\frac{u(r,x)}{u_{\phi}(x)} = f\left(\frac{r}{x+x_0}\right)$$

The "analytical origin" results from an analytical extension of the established-flow pattern into and beyond the limits of the initial region. This origin does not necessarily coincide with the location of the orifice because of the markedly different conditions in the initial region; in fact, it may be expected always to lie below the orifice because of the faster expansion rate in the zone of flow establishment.

The similarity criterion requires a linear spread of the Gaussian profiles with distance from the analytical origin,

$$\sigma = c(x+x_0) \quad (7)$$

and hence

$$\frac{u(r,x)}{u_{\phi}(x)} = e^{-r^2/2c^2(x+x_0)^2} \quad (8)$$

If the density defect due to the air bubbles is also described by a Gaussian distribution curve similar with respect to the analytical origin

$$\Delta \rho(r,x) = \Delta \rho_{\phi}(x) e^{-r^2/2\alpha^2 c^2(x+x_0)^2}$$

(the rate of spread of the bubble stream and of the mixture velocity profiles being proportional to each other) there results

$$\frac{\rho_m(r,x)}{\rho_w} = \frac{\rho_w - \Delta \rho(r,x)}{\rho_w} = 1 - \frac{\Delta \rho_{\phi}(x)}{\rho_w} e^{-r^2/2\alpha^2 c^2(x+x_0)^2} \quad (9)$$

From the equation of continuity for the air bubble stream

$$\frac{Q_0}{\bar{u}_b} = \int_0^{\infty} \Delta \rho(r,x) 2\pi r dr = 2\pi \alpha^2 c^2 (x+x_0)^2 \Delta \rho_{\phi}(x)$$

follows that

$$\frac{\Delta \rho_{\phi}(x)}{\rho_w} = \left(\frac{\rho_a^{atm}}{\rho_w}\right) \frac{\psi_0}{2\pi \alpha^2 c^2 \bar{u}_b (x+x_0)^2} \approx \frac{1}{50} \frac{\psi_0}{\bar{u}_b (x+x_0)^2}$$

since the density ratio is about 800 and the rate of spread (αc) of the bubble stream is of the order of magnitude of 0.1. From this expression and eq.(9) it is therefore seen that the mixture density can only differ considerably from the water density for air supply rates ψ_0 much larger than the product

$\bar{u}_b (x + x_0)^2$. However, \bar{u}_b is of the order of magnitude of 1 m/s, and outside the initial region ($x + x_0$) is usually larger than 1 m. Hence significant density variations are to be expected only for air supply rates much in excess of 1 m³/s, which is far beyond any practicable limit. Outside the initial region the variations in density can therefore be safely neglected.

The assumed velocity profiles can now be integrated to yield the mass flux

$$\left. \begin{aligned} Q(x) &= \int_0^{\infty} \rho_m(r, x) u(r, x) 2\pi r dr = 2\pi \rho_w u_{\xi}(x) \int_0^{\infty} e^{-r^2/2c^2(x+x_0)^2} r dr \\ Q(x) &= 2\pi \rho_w u_{\xi}(x) c^2 (x+x_0)^2 \end{aligned} \right\} (10)$$

and the momentum flux

$$M(x) = \int_0^{\infty} \rho_m(r, x) u^2(r, x) 2\pi r dr = \pi \rho_w u_{\xi}^2(x) c^2 (x+x_0)^2 \quad (11)$$

Comparison of the expressions for the momentum flux in eqs.(6) and (11), based upon the assumption of negligible pressure differences in the zone of established flow, leads to an expression for the centerline velocity

$$u_{\xi}(x) = \frac{1}{c(x+x_0)} \sqrt{\frac{-P_{atm} \psi_0}{\pi \rho_w \bar{u}_b} \ln(1-x/h^*)} \quad (12)$$

and substitution of eq.(12) into eq.(10) gives the volume flux ratio

$$\frac{Q(x)/\rho_w}{\psi_0} = 2\pi c(x+x_0) \sqrt{\frac{-P_{atm}}{\pi \rho_w \bar{u}_b} \frac{\psi_0}{\psi_0} \ln(1-x/h^*)} \quad (13)$$

with the mass flux ratio being about 800 times as large. The momentum flux ratio is given by

$$\frac{M(x)}{M_0} = - \left(\frac{P_0}{P_{atm}} \right) \frac{gRT\pi d_0^2/4}{\bar{u}_b \psi_0} \ln(1-x/h^*) \quad (14)$$

Row of orifices (two-dimensional case)

A two-dimensional slot of width b_0 , representing the limiting case for a row of orifices, can be treated in an analog manner. If the mass flux per unit length is Q'_0 and the corresponding atmospheric volume flux ψ'_0 , then the initial momentum is given by

$$M'_0 = \rho_a^{atm} \left(\frac{P_{atm}}{P_0} \right) \frac{\psi'_0{}^2}{b_0} = c_D' U_0 \rho_a^{atm} \psi'_0 \quad (15)$$

and the buoyant force by

$$F'(x) = -\frac{\rho_{atm} \Psi'_0}{\bar{u}_b} \ln(1 - x/h^*)$$

The total momentum flux is now

$$M'(x) = c'_D U_0 \rho_a^{atm} \Psi'_0 - \frac{\rho_{atm} \Psi'_0}{\bar{u}_b} \ln(1 - x/h^*) \quad (16)$$

where the contribution due to the initial momentum flux can again be neglected within the same limits as before.

The assumption of Gaussian velocity profiles similar with respect to the analytical origin x'_0 yields

$$\frac{u'(y, x)}{u'_\xi(x)} = e^{-y^2/2c'^2(x+x'_0)^2} \quad (17)$$

and similarly the density defect is given by

$$\Delta \rho'(y, x) = \Delta \rho'_\xi(x) e^{-y^2/2\alpha'^2 c'^2(x+x'_0)^2}$$

From the equation of continuity for the air bubble stream

$$\frac{Q'_0}{\bar{u}_b} = 2 \int_0^\infty \Delta \rho'(y, x) dy = \sqrt{2\pi} \Delta \rho'_\xi(x) \alpha' c'(x+x'_0)$$

there results, with the density ratio being 800 and the rate of spread ($\alpha' c'$) in the order of magnitude of 0.1,

$$\frac{\Delta \rho'_\xi(x)}{\rho_w} = \left(\frac{\rho_a^{atm}}{\rho_w} \right) \frac{\Psi'_0}{\sqrt{2\pi} \alpha' c' \bar{u}_b (x+x'_0)} \approx \frac{1}{200} \frac{\Psi'_0}{\bar{u}_b (x+x'_0)}$$

and hence

$$\frac{\rho'_m(y, x)}{\rho_w} = 1 - \frac{\Delta \rho'_\xi(x)}{\rho_w} e^{-y^2/2\alpha'^2 c'^2(x+x'_0)^2} \approx 1 - \frac{1}{200} \frac{\Psi'_0}{\bar{u}_b (x+x'_0)} e^{-y^2/2\alpha'^2 c'^2(x+x'_0)^2}$$

Since the discharge rate Ψ'_0 will never reach values much larger than $\bar{u}_b \cdot (x + x'_0)$, which is of the order of magnitude of 1 m²/s outside the initial region, it is seen that the variation in density can again be safely neglected.

Integration over the assumed velocity profiles gives the mass flux

$$\left. \begin{aligned} Q'(x) &= 2 \int_0^\infty \rho'_m(y, x) u'(y, x) dx = 2 \rho_w u'_\xi(x) \int_0^\infty e^{-y^2/2c'^2(x+x'_0)^2} dy \\ Q'(x) &= \sqrt{2\pi} \rho_w u'_\xi(x) c'(x+x'_0) \end{aligned} \right\} \quad (18)$$

and the momentum flux

$$M'(x) = 2 \int_0^{\infty} \rho_m'(y, x) u'(y, x) dx = \sqrt{\pi} \rho_w u_b'^2 c'(x+x_0') \quad (19)$$

For negligible pressure differences, the expressions for the momentum flux in eqs. (16) and (19) yield the centerline velocity

$$u_b'(x) = \sqrt{\frac{-P_{atm} \psi_0' \ln(1-x/h^*)}{\sqrt{\pi} \rho_w \bar{u}_b c'(x+x_0')}} \quad (20)$$

which leads to the volume flux ratio

$$\frac{Q'(x)/\rho_w}{\psi_0'} = \sqrt{\frac{-2\sqrt{\pi} P_{atm} c'(x+x_0') \ln(1-x/h^*)}{\rho_w \bar{u}_b \psi_0'}} \quad (21)$$

and the momentum flux ratio

$$\frac{M'(x)}{M_0'} = - \left(\frac{P_0}{P_{atm}} \right) \frac{gRT b_0}{\bar{u}_b \psi_0'} \ln(1-x/h^*) \quad (22)$$

The assumption of similar Gaussian velocity profiles has thus led to expressions describing the flow in which only the rate of spread c of the profiles, the location x_0 of the analytical origin and the average rate of rise \bar{u}_b of the bubble stream are yet to be determined by experiment.

EXPERIMENTS

In a basin of 8 x 280 x 4.70 m, vertical velocities above single orifices were measured by Ott current meters. The orifice was located at a depth of 4.50 m and hence 0.20 m above the basin floor in most tests, but some measurements have also been made with an 0.2 cm orifice at a depth of 2 m (elevation above floor = 2.70 m) and again at 4.50 m with a false floor around the orifice (zero elevation above floor). Orifices from 0.05 to 0.5 cm in diameter were tested at air discharges up to 6 200 cm³/s. Since the flow is subject to considerable fluctuations, it was found necessary to measure over a period of 5 min at each point. Profiles have been taken along the jet axis (for an example, see Fig.4) and in normal planes at various heights (Fig.6).

In the same basin, a row of 0.1 cm orifices spaced 7.5 cm apart was tested. The air pipe with a total length of 4.50 m was located 4.30 m below the surface. The velocities were measured at midsection. In addition, a row of 0.1 cm orifices spaced 10 cm apart has been investigated in a basin of 1 x 10 x 2 m with the air pipe (total length 1 m) located 2 m below the

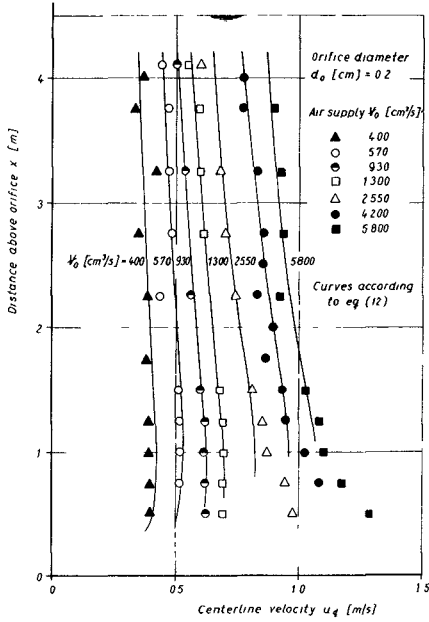


Fig.4 Centerline Velocities above a Single Orifice

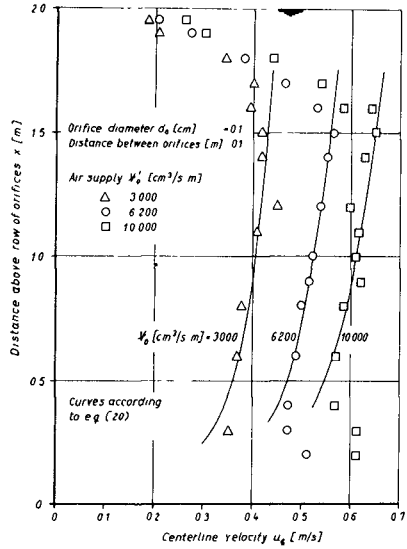


Fig.5 Centerline Velocities above a Row of Orifices

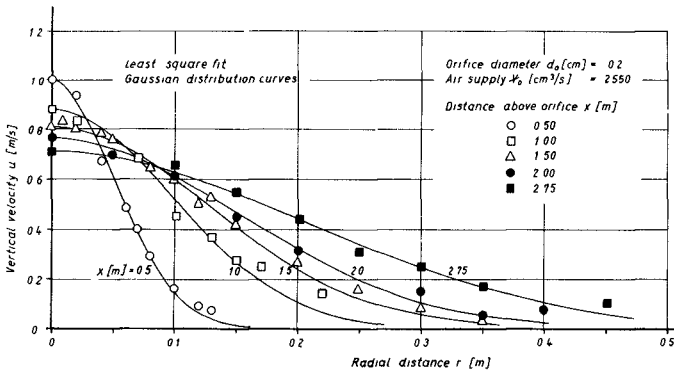


Fig.6 Velocity Profiles above a Single Orifice

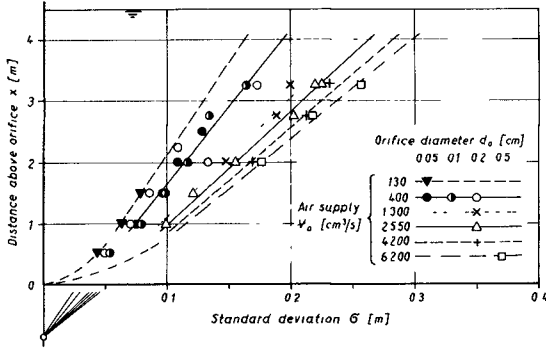


Fig.7 Standard Deviation of Gaussian Velocity Profiles for a Single Orifice

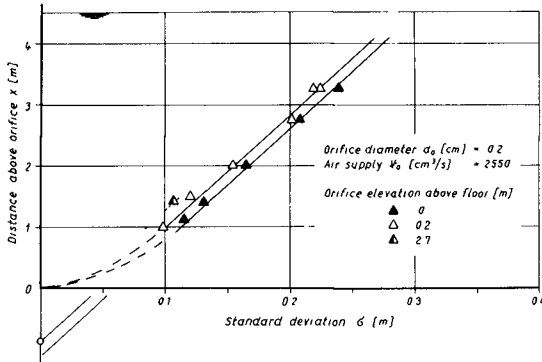


Fig.8 Influence of Orifice Location above the Floor

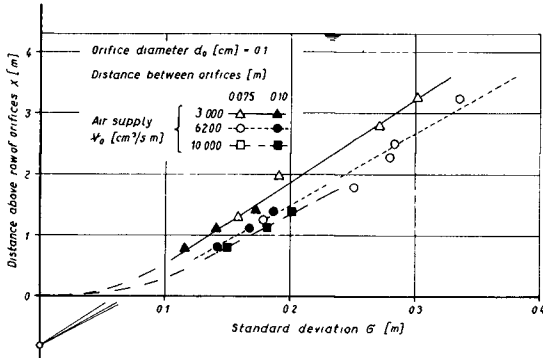


Fig.9 Standard Deviation of Gaussian Velocity Profiles for a Row of Orifices

surface at the basin floor. Fig.5 shows velocity profiles along the jet axis for discharge rates up to 10 000 cm³/s·m.

The average rate of rise \bar{u}_b of the bubble stream in sideways unlimited water was evaluated from density measurements by means of radioisotopes. If a flat, horizontal volume is chosen such that all bubbles have to pass through it, then \bar{u}_b can be determined from the mean density, the dimensions of the volume and the known air supply rate. Figs.11 and 12 show the mean rising speed of bubble streams from various orifices as functions of the air supply for single orifices and rows, respectively. At small air supply rates, for which density measurements become unsatisfactory, but visual observation is possible, time-length measurements have been made.

DISCUSSION OF RESULTS

Gaussian distribution curves are seen (Fig.6) to fit the experimental data well. The standard deviation of the least-square fits increases linearly with height for both single orifices (Fig.7) and rows (Fig.9), which justifies the assumption of similar Gaussian velocity profiles.

From the variation of the standard deviation with height as shown in Figs.7, 8 and 9, the location x_0 of the "analytical origin" results from an extension beyond the initial region. Since x_0 is an artificial aid to compensate for the untraceable conditions in the initial region, it can be expected to depend upon the local orifice geometry and especially to vary with the orifice elevation above the floor (Fig.8). For the normal test arrangement, x_0 was found to be about 0.8 m, independent of the air supply rate. The value of x_0 seems to increase slightly with water depth; however, the measurements allow only an estimate with possible variations of several tenths of a meter. Nevertheless this information is sufficient, since x_0 appears only in the combination $(x + x_0)$ with x always larger than the extent of the initial region, and therefore small variations in x_0 are of little influence upon the results.

The rate of spread c of the velocity profiles, which is determined by the conditions in the region of established flow, is seen to vary with the air supply rate (Fig.10). The parallel shift of the straight lines in Fig.8 shows that it is independent of the local orifice geometry, and Fig.10 indicates independence of orifice size and spacing. The rate of spread increases for both single orifices and rows approximately with the air supply rate to the 0.15 power.

The mean rising speed \bar{u}_b of the bubble stream is shown in Figs.11 and 12. In spite of considerable scatter the results give an indication of the magnitude of \bar{u}_b at least for higher air supply rates. Independent of orifice size, \bar{u}_b increases with the air supply to about the 0.15 power for both single orifices and rows.

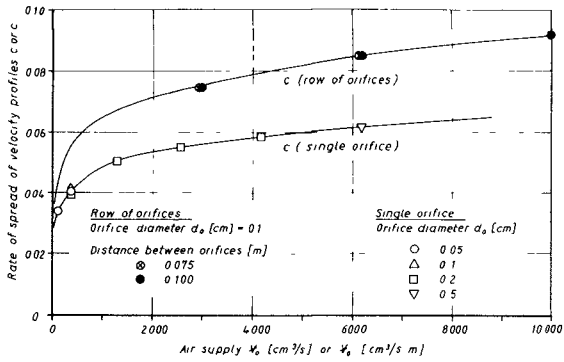


Fig.10 Rate of Spread of the Velocity Profiles

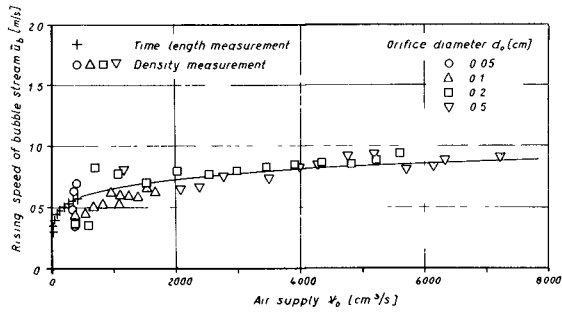


Fig.11 Average Rising Speed of the Bubble Stream from a Single Orifice

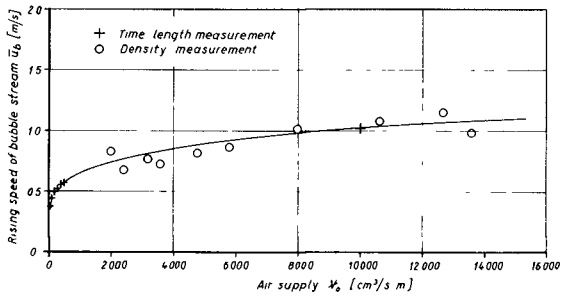


Fig.12 Average Rising Speed of the Bubble Stream from a Row of Orifices

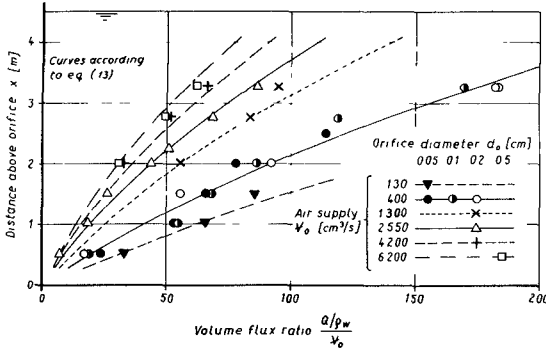


Fig.13 Volume Flux Ratio for a Single Orifice

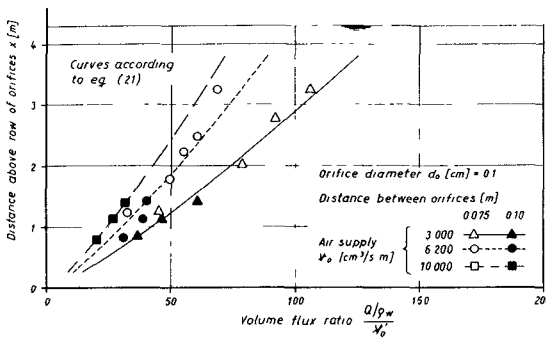


Fig.14 Volume Flux Ratio for a Row of Orifices

With the experimental information about x_0 , c and \bar{u}_0 at hand, the analysis gives expressions for the centerline velocities and the volume flux ratios which can now be compared with the direct experimental results.

For a single orifice, the centerline velocity varies with the air supply rate to the 1/4 power and shows, after a rapid initial growth, a slight decrease with distance from the orifice (Fig.4). The volume flux ratio (Fig.13) increases more than linearly with height and shows a decrease with the air supply rate to the -0.4 power.

The centerline velocity for a row of orifices increases with distance from the orifice at an ever decreasing rate (Fig.5)

and grows with the air supply to the $1/3$ power, which is in agreement with the heat-flow analogy by Taylor [6] and experimental findings of others [3,7]. The volume flux ratio (Fig.14) shows a slightly less than linear increase with height and varies with the air supply to the $-1/2$ power.

In both cases, the measured velocities deviate from the analytical profiles in the initial region and near the free surface, as was to be expected, but in the region of established flow experimental points and analytical curves show good agreement (Figs.4 and 5). Also, the volume flux ratios as determined from integration of the measured velocity profiles and predicted by the analysis show a fair fit for both single orifices (Fig.13) and rows (Fig.14) even close to the orifice.

CONCLUSIONS

Measurements of vertical velocities in the flow field above an orifice discharging air into water show that profiles in horizontal planes can be represented by Gaussian distribution curves with a linear spread in the vertical. This permits an analytical treatment of similar Gaussian velocity distribution curves with proper consideration of the increase in momentum flux with height due to the buoyancy of the air bubble stream, which leads to a description of the flow pattern except for the regions near the orifice and near the free surface. It contains three experimental parameters: the location x_0 of the analytical origin below the orifice, the linear rate of spread c of the velocity profiles, and the mean rising speed \bar{u}_b of the air bubble stream.

While the location x_0 of the analytical origin was found to be 0.8 m independent of the air supply rate, but with possible variations of several $1/10$ of a meter due to depth of submergence and local orifice geometry (mainly orifice elevation above the floor), the rate of spread c of the profiles is independent of orifice size, spacing and geometry. Both the two-dimensional and the axisymmetric rate of spread increase with the air supply to about the 0.15 power. The mean rising speed \bar{u}_b of the bubble stream seems to grow also with the 0.15 power of the air supply independent of orifice size.

With the experimental information about the parameters x_0 , c and \bar{u}_b available, the analysis describes the flow pattern completely and yields in particular the volume flux ratio, which is a criterion for the efficiency of an air-bubble system, in terms of location, water depth and air supply rate. For both single orifices and rows the measured vertical velocities and the volume flux ratios obtained therefrom by integration agree well with the analytical predictions, and it is supposed that

extrapolation to larger water depths and air supplies is permissible. In first approximation this analysis should allow predictions of the volume flux for any air-bubble system, and as a first step towards an analytical framework it may ultimately contribute towards providing a means of correlating model tests and field investigations on air-bubble flows.

ACKNOWLEDGMENTS

The experiments described in this paper have been performed in the towing tank of the Versuchsanstalt für Wasserbau und Schiffbau Berlin by Mr. P. Fischer in the course of a research program on the use of air-bubble systems for reducing silt intrusion into estuaries, conducted for the Wasser- und Schifffahrtsdirektion Kiel.

SYMBOLS

Subscript "o" refers to conditions at the orifice.
Primed symbols refer to the two-dimensional case.

d_o (b_o)	orifice diameter (slot width)
c	rate of spread of velocity profiles
c_D	discharge coefficient
h	water depth
h^*	$h + p_{atm} / \gamma_w$
p	pressure
$r(y)$	radial (sideward) distance from orifice
$u(u_t)$	vertical (centerline) velocity
\bar{u}_b	mean rising speed of air bubble stream
x	vertical distance above orifice
x_o	location of analytical origin
F	buoyant force
M	momentum flux
Q	mass flux
R	gas constant for air
T	absolute temperature
U_o	theoretical exit velocity
Ψ	volume flux
α	ratio of expansion rates for air bubble stream and water jet

$\gamma_w (\gamma_a^{\text{atm}})$	specific weight of water (air at atmospheric pressure)
$\rho_w (\rho_a^{\text{atm}})$	density of water (air at atmospheric pressure)
$\Delta \rho \xi$	density defect at centerline
σ	standard deviation of Gaussian distribution curve

REFERENCES

- [1] Rouse, H., Editor. "Advanced Mechanics of Fluids", John Wiley and Sons, Inc., New York 1959
- [2] Baines, W.D.: "The Principles of Operation of Bubbling Systems", Proc., Symposium on Air Bubbling, Ottawa 1961
- [3] Bulson, P.S.: "Currents Produced by an Air Curtain in Deep Water", The Dock and Harbour Authority, May 1961
- [4] Siemes: "Gasblasen in Flussigkeiten", Chemie-Ingenieur-Technik 26 (1954)
- [5] Silberman, E. "Production of bubbles by the disintegration of gas jets in liquid", Proc., 5th Midwestern Conference on Fluid Mechanics, U of Mich., 1957
- [6] Taylor, Sir G.: "The action of a surface current used as a breakwater", Proc. Royal Society A, Vol. 231, 1955
- [7] Kurihara, M: "On the Study of a Pneumatic Breakwater in Japan", Coastal Engineering in Japan, Japan S.C.E., Vol. VIII, 1965
- [8] Murota, A. and Muraoka, K: "Turbulent Diffusion of the Vertically Upward Jet", Proc., 12th IAHR Congress, Fort Collins 1967